Mathematics and Systems Science 2025, 3(2), 3359.
https://doi.org/10.54517/mss3359

Article

Co-dynamics of measles and hand-foot-mouth disease

Guichen Lu[1,2,*], Langhao Dou[1], Yifan Miao[1], Lixiang Chen[1]

[1] School of Science, Chongqing University of Technology, Chongqing 400054, China

[2] School of Mathematics Sciences, University of Electronic Science and Technology of China, Chengdu 611731, China

*** Corresponding author:** Guichen Lu, guichenlu@cqut.edu.cn

CITATION

Lu G, Dou L, Miao Y, Chen L. Co-dynamics of measles and hand-foot-mouth disease. Mathematics and Systems Science. 2025; 3(2): 3359. https://doi.org/10.54517/mss3359

ARTICLE INFO

Received: 28 February 2025
Accepted: 3 April 2025
Available online: 14 April 2025

Abstract: This study develops two compartmental models to analyze the co-dynamics between measles and hand, foot, and mouth disease (HFMD): a four-compartment model and a seven-compartment HFMD-Measles co-infection model. For the four-compartment model, we systematically analyzed the co-dynamics of measles and hand, foot, and mouth disease (HFMD), and employed the next-generation matrix method to calculate the basic reproduction number of measles and that of HFMD. Through the analytical study of these two types of basic reproduction numbers, we rigorously determined the existence of the disease equilibrium points, with their quantitative relationship were clearly illustrated through graphical representations. The global asymptotic stability of these equilibria is established by applying LaSalle invariance principle, with stability regions of the four equilibrium points precisely defined. The analysis reveals that within the stability region of the disease-free equilibrium, both diseases will eventually die out, preventing any outbreaks. In the stability region corresponding to the measles equilibrium, HFMD is eliminated while measles remains endemic. Conversely, in the stability region of the HFMD-only equilibrium, measles dies out whereas HFMD persists. Finally, within the stability region of the coexistence equilibrium, both diseases persist and become endemic. Numerical simulations further validate the consistency and reliability of these theoretical results. For the seven-compartment infectious disease model, we calculated the basic reproduction number and verified the threshold theorem. We derived the conditions for both local and global asymptotic stability of the disease-free equilibrium. In particular, the disease-free equilibrium is locally stable when the basic reproduction number is less than one, and we also provided conditions for its global stability. Model validation is performed by fitting empirical data from China on HFMD and measles cases.

Keywords: co-infection; basic reproduction number; LaSalle invariance principle; global asymptotic stability

1. Introduction

Measles, caused by the measles virus, spreads through respiratory droplets and presents symptoms such as fever, cough, runny nose, conjunctivitis, and rash. Severe cases may lead to pneumonia or encephalitis, and the virus can temporarily suppress immune function, even post-vaccination with live attenuated vaccines [1–4]. To better understand and control measles spread, researchers widely use mathematical modeling. These studies reveal transmission mechanisms and inform prevention strategies. For example, Azam et al. [5] integrated vaccine supply chains with transmission models, highlighting benefits of non-cold-chain vaccine use in resource-limited areas. Xue et al.

[6] developed a model with network structures and vaccine immunity decay, analyzing random and scale-free networks to show their impact on transmission. Ibrahim et al. [7] created a seasonal model with two-dose vaccination, using the basic reproduction number to predict and control outbreaks. Peter et al. [8] proposed a seven-category population model, studying vaccination and contact rates to guide public health policies. Ahmad et al. [9] built an SVEITR model with time-dependent vaccination and treatment strategies, optimizing infection reduction and public health outcomes. Berhe et al. [10] used Lyapunov functions to analyze global stability, supporting long-term control. Furthermore, Arsal [11] reviewed various refined measles models that integrated vaccination, co-infection, age structure, and seasonal factors, enhancing prediction accuracy based on limited epidemiological data.

Hand, Foot, and Mouth Disease (HFMD) is a common infectious disease caused by enteroviruses, primarily affecting children under five. It spreads through close contact, respiratory droplets, and the fecal-oral route. Symptoms include fever, oral ulcers, and skin rashes. While most cases are mild, some can lead to severe complications like meningitis and may be life-threatening. Ma et al. [12] developed a transmission model for HFMD, treating asymptomatic carriers as an independent group and incorporating a periodic infection rate. They applied this model to fit HFMD data from Shandong Province over more than two years. Wang et al. [13, 14] explored the impact of environmental pollution and vaccination on HFMD transmission, analyzing the model's dynamics and fitting it to data from mainland China between 2010 and 2014, revealing the significant role of environmental contamination. Zhang et al. [15] examined the effect of behavioral changes on HFMD transmission and found that substantial behavioral modifications significantly impact disease dynamics.

Co-infection, the simultaneous or sequential infection by multiple pathogens, has gained increasing attention in infectious disease research. Studies have explored the interaction between HIV and measles virus, highlighting their combined immunosuppressive effects, which lead to immune exhaustion and alter transmission dynamics [16]. Berhe et al. [17] developed a dynamic model for co-infection of measles and dysentery, aiming to minimize infection rates and control costs. Zhang et al. [18] examined co-infection between measles and hand, foot, and mouth disease (HFMD), showing that measles-induced immune suppression can worsen HFMD symptoms, while HFMD may affect measles progression. Such co-infections can enhance viral transmission, raising epidemic risks.

This study focuses on two major communicable diseases, measles and hand, foot, and mouth disease (HFMD), both primarily transmitted through human-to-human contact. The aim is to conduct an in-depth analysis of their transmission patterns, characteristics of susceptible populations, and effective prevention strategies, thereby revealing the key factors that influence the spread and management of these diseases. To more accurately simulate the transmission process, we designed a multi-compartment infectious disease model controlled by ordinary differential equations, dividing the population into five compartments. Additionally, we specifically examine the potential interactions between measles and HFMD by introducing variants of the model to reflect the complex relationship between these

two diseases during actual transmission. This comprehensive analytical approach not only increases the model's complexity but also makes it more aligned with real-world scenarios, thus providing a more targeted scientific basis for the formulation of infectious disease prevention and control strategies, and advancing the development of infectious disease modeling research.

The paper is organized as follows: Section 2 presents the co-infection model for measles and hand, foot, and mouth disease. In Section 3, we analyze the basic reproduction numbers and the existence, local, and global stability of equilibria of a four-compartment SI_hI_mR model. In Section 4, we calculate basic reproduction numbers for a seven-compartment $SI_hI_mImhR_hR_mR_{mh}$ model and validate stability conditions for the disease-free equilibrium. Section 5 describes the numerical methods and validates the model using empirical data from China on HFMD and measles. Finally, Section 6 provides a discussion and conclusion.

2. Model formulation

To depict the impact of the interaction between measles patients and hand, foot, and mouth disease (HFMD) patients on the immune system, considering the similarity in clinical symptoms of the two diseases, the entire population of a region is divided into four compartments: Susceptible (S), HFMD patients not infected with measles virus (I_h), measles patients and patients infected with both viruses (I_m), and Recovered (R). Let $S(t)$, $I_h(t)$, $I_m(t)$, and $R(t)$ represent the number of individuals in each compartment at time t. Additionally, the total population at time t is denoted as $N(t) = S(t) + I_h(t) + I_m(t) + R(t)$.

In considering the interaction between the two virus types within the host, we propose the following assumptions:

(A_1). The population is homogeneous, ensuring equal contact opportunities for all individuals, and a host may contract one or multiple diseases.

(A_2). Susceptible individuals become infected through contact with infected individuals. The probability of transmission from an infected individual to a susceptible individual is denoted by β_1 per unit time. Both hand, foot, and mouth disease (HFMD) and measles patients transmit the infection at the same rate β_2.

(A_3). Considering the high virulence of the measles virus, we assume that there is a risk of co-infection between measles patients and HFMD patients. Specifically, when an HFMD patient contacts a measles patient, the probability of transitioning to an HFMD-measles co-infected state is τ per unit time.

(A_4). For the purposes of this model, recurrence of either HFMD or measles in infected patients is not considered.

(A_5). All parameters are non-negative, based on their biological relevance.

Based on these assumptions and the transmission dynamics of both viruses, we outline the corresponding flowchart as follows(**Figure 1**):

As illustrated in **Figure 1**, the system can be mathematically described by the following four governing equations:

$$\begin{cases} S' = \Lambda - \beta_1 S I_h - \beta_2 S I_m - \mu S, \\ I_h' = \beta_1 S I_h - (\theta_1 + d_1 + \mu) I_h - \tau I_h I_m, \\ I_m' = \beta_2 S I_m + \tau I_h I_m - (\theta_2 + d_2 + \mu) I_m, \\ R' = \theta_1 I_h + \theta_2 I_m - \mu R \end{cases} \tag{1}$$

where the descriptions of the model parameters can be found in **Table 1**.

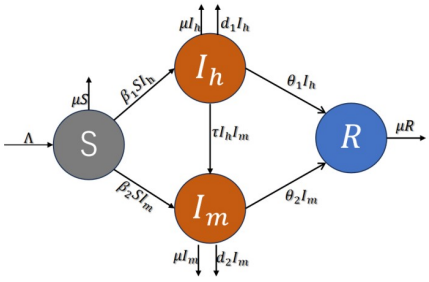

Figure 1. The transmission compartment diagram of the SI_hI_mR model.

Table 1. Definitions of Parameters in the SI_hI_mR model.

Parameter	Description
Λ	Constant Recruitment Rate
d_1	Mortality rate due to hand, foot, and mouth disease
μ	Natural mortality rate
d_2	Mortality rate due to measles
β_1	Transmission rate from susceptible individuals to HFMD patients
θ_1	Recovery rate for hand, foot, and mouth disease
β_2	Transmission rate from susceptible individuals to measles patients
θ_2	Recovery rate for measles
τ	Effective transmission rate from HFMD cases to Measles patients

Since the I_m compartment in model (1) accommodates both pure measles patients and HFMD-measles co-infected patients, it becomes difficult to clearly define the interaction between the two diseases. To address this, we introduce a new compartment, I_{mh}, specifically designed to depict the co-infection of measles and HFMD. Additionally, to more accurately describe the immune states following independent immunity and co-infection, inspired by Chen et al. [19], we supplement model (1) with the following assumptions.

(A_6). Based on assumption (A_2), we assume that when hand, foot, and mouth disease (HFMD) patients come into contact with measles patients, there is a certain probability that the HFMD patients will contract measles, thus becoming co-infected with both HFMD and measles. These co-infected individuals will then enter compartment I_{mh} at a specific rate. Specifically, we assume that, each HFMD patient has a probability of τ_1 per unit time of transforming into a HFMD-Measles co-infected patient upon contact with a measles patient.

(A_7). Measles patients experience a temporary weakening of the immune system due to viral infection. During this period, if they are exposed to secretions,

contaminants, or high-risk environments (such as childcare facilities) of hand, foot, and mouth disease patients, and fail to strictly implement hand hygiene or environmental disinfection, they may subsequently contract hand, foot, and mouth disease at a conversion rate of τ_2, resulting in co-infection with both measles and hand, foot, and mouth disease.

(A_8). When infected individuals are permanently excluded from the susceptible population due to recovery and immunity, effective isolation, or death, they are assigned to three distinct immunity compartments based on the type of infection. The immunity compartment for hand, foot, and mouth disease (HFMD) is assigned to those recovering from HFMD (R_h), while the immunity compartment for measles is assigned to those recovering from measles (R_m). Individuals recovering from a co-infection (i.e., infection with both HFMD and measles viruses) are assigned to the dual immunity compartment (R_{mh}). Specifically, single-infection individuals, I_h and I_m, enter the R_h compartment from HFMD infection and the R_m compartment from measles infection with recovery rates θ_1 and θ_2, respectively. co-infection individuals, I_{mh}, enter the R_{mh} compartment with an overall recovery rate θ_3, acquiring permanent immunity to both diseases.

The transmission flow chart is established based on the above assumptions (**Figure 2**).

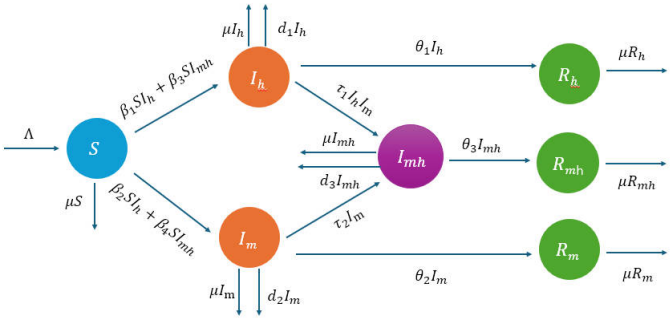

Figure 2. The transmission compartment diagram of the $SI_hI_mI_{mh}R_mR_hR_{mh}$ model.

The system is mathematically represented by seven governing equations, as shown in **Figure 2**.

$$\begin{cases} S' = \Lambda - \beta_1 S I_h - \beta_2 S I_m - (\beta_3 + \beta_4) S I_{mh} - \mu S \\ I_h' = \beta_1 S I_h + \beta_3 S I_{mh} - (\theta_1 + d_1 + \mu) I_h - \tau_1 I_h I_m \\ I_m' = \beta_2 S I_m + \beta_4 S I_{mh} - (\theta_2 + d_2 + \mu) I_m - \tau_2 I_m \\ I_{mh}' = \tau_1 I_h I_m + \tau_2 I_m - (\theta_3 + d_3 + \mu) I_{mh} \\ R_h' = \theta_1 I_h - \mu R_h \\ R_m' = \theta_2 I_m - \mu R_m \\ R_{mh}' = \theta_3 I_{mh} - \mu R_{mh} \end{cases} \tag{2}$$

where the descriptions of the model parameters can be found in **Tables 1** and **2**.

Table 2. Definition of Parameters for the $SI_hI_mI_{mh}R_mR_hR_{mh}$ model.

Parameter	Description
β_3	Transmission rate of susceptibles to HFMD due to HFMD-Measles cases
β_4	Transmission rate of susceptibles to measles due to HFMD-Measles cases
τ_1	Transition rate from HFMD patients to HFMD-Measles co-infection
τ_2	Transition rate from Measles patients to HFMD-Measles co-infection
θ_3	Recovery rate of patients with HFMD-Measles co-infection

Model (2) improves disease representation in two key aspects: First, it introduces an HFMD-Measles co-infection compartment to quantify disease interactions. Second, it refines the classification of recovered individuals based on the distinct recovery characteristics of the two infectious diseases, categorizing them into R_h (HFMD-recovered), R_m (Measles-recovered), and R_{mh} (Recovered from both). Compared to model (1), which consolidates all recovered individuals into a single R compartment, this model adopts a differentiated approach to recovery modeling, aligning more closely with clinical realities.

3. Analysis of the the SI_hI_mR infectious disease model

In this section, we investigate the existence and stability of equilibrium points in model (1). By calculating the basic reproduction number of the model, we establish the conditions for the existence of various equilibrium points. Additionally, we analyze the stability of these equilibrium points using the Lyapunov-LaSalle stability theorem.

Let $x = (S, I_h, I_m, R) \in R_+^4$,$f(x) = (f_1(x), f_2(x), f_3(x), f_4(x))^T$ where

$$\begin{cases} f_1(x) = \Lambda - \beta_1 S I_h - \beta_2 S I_m - \mu S \\ f_2(x) = \beta_1 S I_h - M_1 I_h - \tau I_h I_m \\ f_3(x) = \beta_2 S I_m + \tau I_h I_m - M_2 I_m \\ f_4(x) = \theta_1 I_h + \theta_2 I_m - \mu R \end{cases}$$

Here $M_1 = \theta_1 + d_1 + \mu$,$M_2 = \theta_2 + d_2 + \mu$.

The system described in equation (1) can be reformulated as follows:

$$\dot{x} = f(x) \tag{3}$$

The set Ω is defined as follows:

$$\Omega = \{(S, I_h, I_m, R) \in R_4^+ | 0 \leq S, I_h, I_m, R, S + I_h + I_m + R \leq \frac{\Lambda}{\mu}\}.$$

3.1. Invariance of Model (1)

Theorem 1. *The set Ω is positively invariant with respect to system (1) and serves as a global attractor for the system.*

Proof. (1) For any $x = (S, I_h, I_m, R) \in R_+^4$, it is easy to see that

$$\begin{aligned} &f_1(x) \mid_{S=0} = \Lambda \geq 0, \\ &f_2(x) \mid_{I_h=0} = 0, \\ &f_3(x) \mid_{I_m=0} = 0, \\ &f_4(x) \mid_{R=0} = \theta_1 I_h + \theta_2 I_m \geq 0 \end{aligned}$$

From the principle of invariance [20,21], it follows that the system preserves the non-negativity of its states, i.e., $x(t) \geq 0$ for all $t \geq 0$ whenever $x(0) \geq 0$. This property ensures that R_+^4 is a positively invariant set for the system (1).

(2) Since the total population $N(t) = S(t)+I_h(t)+I_m(t)+R(t)$, and considering the system described in (1) along with the positive invariance established in the first part, it follows that

$$N'(t) = \Lambda - \mu N(t) - d_1 I_h - d_2 I_m \leq \Lambda - \mu N(t),$$

According to the comparison theorem [21], for any $t \geq 0$, we have

$$N(t) \leq \frac{\Lambda}{\mu} - e^{-\mu t}(\frac{\Lambda}{\mu} - N(0))$$

From (1), it is known that when $N(0) \leq \frac{\Lambda}{\mu}$, for all $t \geq 0$, $N(t) \leq \frac{\Lambda}{\mu}$. Consequently, when $x(0) \in \Omega$, for all $t \geq 0$, $x(t) \in \Omega$.

(3) Based on the proof process of (2), we have

$$N'(t) \leq \Lambda - \mu N(t),$$

Furthermore, we obtain

$$\limsup_{t \to +\infty} N(t) \leq \frac{\Lambda}{\mu},$$

From this, it follows that the set Ω constitutes a global attractor of the system (1). □

3.2. Basic reproduction number and existence of equilibria

3.2.1. Basic reproduction number

The basic reproduction number is defined as the average number of secondary infections generated by a single infectious individual in a fully susceptible population. From system (1), it is evident that the system always has a disease-free equilibrium point $E_0 = (\frac{\Lambda}{\mu}, 0, 0, 0)$. Let $u = (I_h, I_m)$ denote the infected compartments, and the corresponding infected subsystem can be described as :

$$\begin{aligned} {I_h}' &= \beta_1 S I_h - M_1 I_h - \tau I_h I_m, \\ {I_m}' &= \beta_2 S I_m + \tau I_h I_m - M_2 I_m \end{aligned} \tag{4}$$

Taking

$$\mathcal{F}(u) = (\beta_1 SI_h, \beta_2 SI_m)^T,$$
$$\mathcal{V}(u) = (M_1 I_h + \tau I_h I_m, M_2 I_m - \tau I_h I_m)^T$$

system (4) can therefore be rewritten as:

$$u' = \mathcal{F}(u) - \mathcal{V}(u). \tag{5}$$

Therefore, the Jacobian matrices for $\mathcal{F}$ and $\mathcal{V}$ at the equilibrium point E_0 are derived as follows:

$$F = D\mathcal{F}(E_0) = \begin{bmatrix} \beta_1 S_0 & 0 \\ 0 & \beta_2 S_0 \end{bmatrix}, V = D\mathcal{V}(E_0) = \begin{bmatrix} M_1 & 0 \\ 0 & M_2 \end{bmatrix},$$

where $S_0 = \frac{\Lambda}{\mu}$.

Let FV^{-1} denote the next-generation matrix, with $\rho(FV^{-1})$ representing its spectral radius. Using the next-generation matrix method [22, 23], the basic reproduction number for the system (1) is given by:

$$R_0 = \rho(FV^{-1}) = \max\{R_0^h, R_0^m\},$$

where $R_0^h = \frac{\beta_1 \Lambda}{\mu M_1}$ and $R_0^m = \frac{\beta_2 \Lambda}{\mu M_2}$ are the basic reproduction numbers for hand-foot-mouth disease and measles, respectively.

In the co-infection model, R_0 is defined by the dominant disease, reflecting the average number of secondary infections caused by a single infectious individual in a fully susceptible population.

Furthermore, we define an additional parameter R_0^{mh} as follows:

$$R_0^{mh} = 1 + \frac{M_1 M_2}{\tau \Lambda}(R_0^h - R_0^m).$$

The comparative analysis of basic reproduction numbers reveals distinct transmission patterns between the two diseases. When the threshold parameter R_0^{mh} exceeds unity ($R_0^{mh} < 1$), measles demonstrates superior transmission capability compared to hand-foot-mouth disease, as evidenced by the relationship $R_0^h < R_0^m$. Conversely, the condition $R_0^{mh} > 1$ indicates a stronger transmission potential for hand-foot-mouth disease, characterized by $R_0^h > R_0^m$. The critical threshold $R_0^{mh} = 1$ represents an equilibrium state where both diseases exhibit equivalent transmission dynamics, maintaining a balanced epidemiological relationship without dominance of either disease.

3.2.2. Existence of equilibria

Let $f(x) = 0$. Through straightforward calculations, the following conclusions can be easily derived:

Theorem 2. *(1) For $R_0 < 1$, the system described by Equation (1) has only the disease-free equilibrium point E_0.*

(2) When $R_0^h < 1 < R_0^m$, system (1) possesses both the disease-free equilibrium point

E_0 and the measles endemic equilibrium point $E_m^* = (S_m^*, 0, I_{mm}^*, R_m^*)$, where $S_m^* = \frac{M_2}{\beta_2}, I_{mm}^* = \frac{\mu}{\beta_2}(R_0^m - 1)$ and $R_m^* = \frac{\theta_2}{\beta_2}(R_0^m - 1)$.
(3) Given that $0 < R_0^m < 1 < R_0^h < R_0^{mh}$, system (1) includes only the disease-free equilibrium point E_0 and the hand-foot-mouth disease endemic equilibrium point $E_h^* = (S_h^*, I_{hh}^*, 0, R_h^*)$, where $S_h^* = \frac{M_1}{\beta_1}$, $I_{hh}^* = \frac{\mu}{\beta_1}(R_0^h - 1)$ and $R_h^* = \frac{\theta_1}{\beta_1}(R_0^h - 1)$.
(4) Under the condition that $1 < R_0^h < R_0^m$ or $1 < R_0^m < R_0^h < R_0^{mh}$ or $1 < R_0^{mh} < R_0^m < R_0^h$, system (1) has the equilibrium points E_0, E_m^* and E_h^*.
(5) If $0 < R_0^m < 1 < R_0^{mh} < R_0^h$, the system described by equation (1) admits the equilibrium points E_0, E_h^* and $E^* = (S^*, I_h^*, I_m^*, R^*)$, where the components S^*, I_m^*, I_h^*, and R^* are explicitly defined by $S^* = \frac{\Lambda^2\tau}{\mu M_1 M_2(R_0^h - R_0^m) + \mu\tau\Lambda}$, $I_m^* = \frac{\Lambda M_1(R_0^h - R_0^{mh})}{\tau\Lambda - M_1 M_2(R_0^m - R_0^h)}$, $I_h^* = \frac{\tau\Lambda M_2(R_0^m - 1) + M_1 M_2^2(R_0^m - R_0^h)}{(M_1 M_2(R_0^m - R_0^h) - \tau\Lambda)\tau}$, $R^* = \frac{\theta_1}{\mu} I_h^* + \frac{\theta_2}{\mu} I_m^*$.
(6) Under the condition $1 < R_0^m < R_0^{mh} < R_0^h$, the system (1) admits equilibrium points E_0, E_h^*, E_m^* and E^*.

Based on the aforementioned analysis, the existence of equilibrium solutions with respect to the parameters R_0^h and R_0^m can be systematically summarized and illustrated in **Figure 3**.

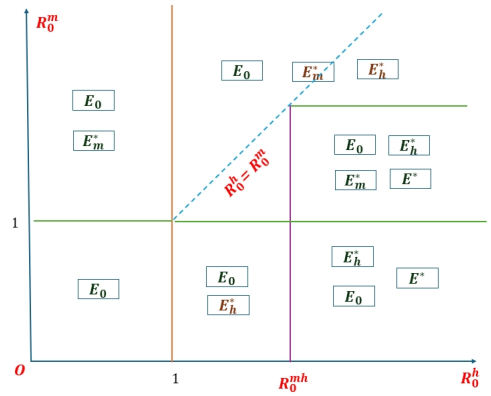

Figure 3. Existence regions of equilibria E_0, E_h^*, E_m^* and E^* of the SI_hI_mR model.

According to **Figure 3**, the existence of equilibrium points depends on the relationship between the basic reproduction number of measles (R_0^m) and that of hand, foot, and mouth disease (R_0^h). When R_0^m dominates, i.e.,

$$(R_0^h, R_0^m) \in \Omega_{E_m^*} = \{(R_0^h, R_0^m) \in R_+^2 \mid 0 < R_0^h < 1 < R_0^m\},$$

only the measles endemic equilibrium E_m^* exists. Conversely, when R_0^h dominates, i.e.,

$$(R_0^h, R_0^m) \in \Omega_{E_h^*} = \{(R_0^h, R_0^m) \in R_+^2 \mid 0 < R_0^m < 1 < R_0^h\},$$

only the HFMD endemic equilibrium E_h^* exists. When

$$(R_0^h, R_0^m) \in \Omega_{E_{mh}^*} = \{(R_0^h, R_0^m) \in R_+^2 \mid R_0^h, R_0^m > 1\},$$

both the measles endemic equilibrium E_m^* and the HFMD endemic equilibrium E_h^*

coexist. Finally, when

$$(R_0^h, R_0^m) \in \Omega_{E^*} = \{(R_0^h, R_0^m) \in R_+^2 \mid 0 < R_0^m < R_0^{mh} < R_0^h\},$$

the coexisting measles-HFMD endemic equilibrium E^* emerges. These results indicate that the disease transmission dynamics exhibit significant variations across different parameter regions.

3.3. Stability analysis of SI_hI_mR model (1)

This section aims to explore the system's dynamic characteristics by thoroughly assessing the stability of its equilibrium points. Utilizing LaSalle's invariance principle, we conduct a methodical investigation into the stability features of these steady states. This analytical approach offers a reliable method for predicting the system's asymptotic behavior.

To formulate the Krasovkii-LaSalle invariance principle in [21,23,24], we consider a dynamical system characterized by the following autonomous differential equation:

$$x' = f(x) \tag{6}$$

Under the assumption that the system possesses an equilibrium point x^*, the LaSalle invariance principle can be formally expressed as follows.

Theorem 3. *For system (6), if there exists a continuously differentiable function $V : \mathbb{R}^n \to \mathbb{R}$ that is positive definite and radially unbounded, and its time derivative satisfies $V'(x) \leq 0$ for all $x \in \mathbb{R}^n$, then the equilibrium point x^* is globally asymptotically stable, provided that the set $\mathcal{S} = \{x \in \mathbb{R}^n \mid \dot{V}(x) = 0\}$ contains only $x = x^*$.*

Based on Theorem 3, we can derive the following significant conclusion:

Theorem 4. *Let $V : \mathbb{R}^n \to \mathbb{R}$ be a function satisfying the following conditions:*

(H_1) *$V(x)$ is positive definite and radially unbounded,*

(H_2) *$V'(x) \leq 0$ holds for all $x \in \mathbb{R}^n$,*

(H_3) *the only solution to (6) under $V'(x) = 0$ is $x = x^*$ for all $t \geq 0$.*

Then, the equilibrium point x^* of system (6) is globally asymptotically stable.

3.3.1. Stability analysis of the disease-free equilibrium point E_0

According to the research results of Driessche et al. [22], the following threshold theorem can be derived.

Theorem 5. *When the basic reproduction number $R_0 < 1$, the disease-free equilibrium point E_0 of the system (1) is locally asymptotically stable within the domain Ω. Conversely, when $R_0 > 1$, the equilibrium point E_0 becomes unstable.*

Proof. To assess the stability characteristics of the dynamical system represented by

Equation (1), we evaluate the Jacobian matrix at the disease-free equilibrium state E_0:

$$J_0 = Df(E_0) = \begin{bmatrix} -\mu & -\frac{\beta_1\Lambda}{\mu} & -\frac{\beta_2\Lambda}{\mu} & 0 \\ 0 & \frac{\beta_1\Lambda}{\mu} - M_1 & 0 & 0 \\ 0 & 0 & \frac{\beta_2\Lambda}{\mu} - M_2 & 0 \\ 0 & \theta_1 & \theta_2 & -\mu \end{bmatrix}.$$

The eigenvalues of J_0 are given by:

$$\lambda_1 = \lambda_2 = -\mu,\ \lambda_3 = \frac{\beta_1\Lambda}{\mu} - M_1 = M_1(R_0^h - 1),\ \lambda_4 = \frac{\beta_2\Lambda}{\mu} - M_2 = M_2(R_0^m - 1).$$

Therefore, all eigenvalues exhibit negative values when the basic reproduction number satisfies $R_0 < 1$. However, when $R_0 > 1$, this condition indicates that either $R_0^h > 1$ or $R_0^m > 1$. As a result, at least one of the eigenvalues (λ_3 or λ_4) becomes positive, demonstrating the instability of the disease-free equilibrium point E_0. □

Theorem 6. *The disease-free equilibrium E_0 of the system defined by (1) possesses global asymptotic stability in the domain Ω if and only if the basic reproduction number $R_0 < 1$.*

Proof. Following Theorem 5, the instability of the disease-free equilibrium E_0 is guaranteed when $R_0 > 1$. Thus, the remaining task is to prove the global asymptotic stability of E_0 for the case where $R_0 < 1$.

To analyze the global asymptotic stability of E_0 of the system described by Equation (1), we construct the Lyapunov function:

$$V_0(t) = V_0(S(t), I_h(t), I_m(t)) = S^0 g(\frac{S}{S^0}) + I_h + I_m$$

where $g(u) = u - 1 - \ln u$.

By computing the total derivative of $\frac{dV_0}{dt}$ along the trajectories of the system governed by Equation (1):

$$\begin{aligned} \dot{V}_0(t) = \frac{d}{dt}V_0(t) &= (1 - \frac{S^0}{S})\frac{dS}{dt} + \frac{dI_h}{dt} + \frac{dI_m}{dt} \\ &= (\frac{\Lambda\beta_1}{\mu} - M_1)I_h + (\frac{\Lambda\beta_2}{\mu} - M_2)I_m + \Lambda(2 - \frac{S}{S_0} - \frac{S_0}{S}) \\ &= M_1 I_h(R_0^h - 1) + M_2 I_m(R_0^m - 1) + \Lambda(2 - \frac{S}{S_0} - \frac{S_0}{S}). \end{aligned}$$

Since $R_0 = \max\{R_0^h, R_0^m\} < 1$, implying that both $R_0^h < 1$ and $R_0^m < 1$, it follows that $\dot{V}_0(t) \leq 0$. It is evident that $\dot{V}_0(t) = 0$ holds only when $S = S_0, I_h = I_m = 0$ and $R = 0$. By employing LaSalle's Invariance Principle, as formally stated in Theorem 3, we can conclude that the disease-free equilibrium point E_0 of the system (1) is globally asymptotically stable when $R_0 < 1$. □

3.3.2. Stability analysis of the measles endemic equilibrium point E_m^*

Theorem 7. *If $R_0^h < 1 < R_0^m$ or $1 < R_0^h < R_0^m$ or $1 < R_0^{mh} < R_0^m < R_0^h$, the measles endemic equilibrium point E_m^* of the system (1) is locally and globally asymptotically stable. However, if $1 < R_0^m < R_0^{mh}$ and $1 < R_0^m < R_0^h$, E_m^* becomes*

unstable.

Proof. We construct the following Lyapunov function:

$$V_m(t) = V_m(S(t), I_h(t), I_m(t)) = S_m^* g(\frac{S}{S_m^*}) + I_h + I_{mm}^* g(\frac{I_m}{I_{mm}^*}).$$

Next, we compute the total derivative of $V_m(t)$ along the trajectories of the system (1):

$$\begin{aligned}\dot{V}_m(t) = \frac{d}{dt}V_m(t) &= (1 - \frac{S_m^*}{S})\frac{dS}{dt} + \frac{dI_h}{dt} + (1 - \frac{I_{mm}^*}{I_m})\frac{dI_m}{dt} \\ &= \Lambda + \mu S_m^* + M_2 I_{mm}^* - (\mu + \beta_2 I_{mm}^*)S \\ &\quad - \Lambda\frac{S_m^*}{S} - (M_1 + \tau I_{mm}^* - \beta_1 S_m^*)I_h.\end{aligned}$$

Given that

$$\begin{aligned}&\mu S_m^* + M_2 I_{mm}^* = S_m^*(\beta_2 I_{mm}^* + \mu) = \Lambda, \\ &M_1 + \tau I_{mm}^* - \beta_1 S_m^* = \frac{1}{M_2 R_0^m}[\Lambda\tau(R_0^m - 1) + M_1 M_2(R_0^m - R_0^h)].\end{aligned}$$

We can conclude that when $R_0^h < 1 < R_0^m$ or $1 < R_0^h < R_0^m$ or $1 < R_0^{mh} < R_0^m < R_0^h$, the total derivative of $\dot{V}_m(t)$ becomes

$$\begin{aligned}\dot{V}_m(t) &= 2\Lambda - (\mu + \beta_2 I_{mm}^*)S - \Lambda\frac{S_m^*}{S} - (M_1 + \tau I_{mm}^* - \beta_1 S_m^*)I_h \\ &\leq 2\Lambda - 2\sqrt{(\mu + \beta_2 I_{mm}^*)\Lambda S_m^*} - \frac{1}{M_2 R_0^m}[\Lambda\tau(R_0^m - 1) + M_1 M_2(R_0^m - R_0^h)]I_h \\ &= -\frac{1}{M_2 R_0^m}[\Lambda\tau(R_0^m - 1) + M_1 M_2(R_0^m - R_0^h)]I_h \\ &= -\frac{\tau\Lambda}{M_2 R_0^m}(R_0^m - R_0^{mh})I_h \leq 0.\end{aligned}$$

Furthermore, it can be deduced that $\dot{V}_m(t) = 0$ only when $S = S_m^*, I_h = 0, I_m = I_{mm}^*$, and $R = R_m^*$. Following the theoretical framework provided by LaSalle's Invariance Principle (as presented in Theorem 3), we can infer that the equilibrium point E_m^* of the system (1) is globally asymptotically stable when $R_0^h < 1 < R_0^m$.
The Jacobian matrix of the system (1) evaluated at the equilibrium point E_m^* is:

$$J_m = J(E_m^*) = \begin{bmatrix} -\frac{\Lambda\beta_2}{M_2} & -\frac{\beta_1 M_2}{\beta_2} & -M_2 & 0 \\ 0 & \frac{\beta_1 M_2}{\beta_2} - \frac{\tau(\Lambda\beta_2 - \mu M_2)}{M_2\beta_2} - M_1 & 0 & 0 \\ \frac{\Lambda\beta_2 - \mu M_2}{M_2} & \frac{\tau(\Lambda\beta_2 - \mu M_2)}{M_2\beta_2} & 0 & 0 \\ 0 & \theta_1 & \theta_2 & -\mu \end{bmatrix}.$$

Let the eigenvalues of the matrix J_m be $\lambda_i (i = 1, 2, 3, 4)$, as follows:

$$\begin{aligned}
&\lambda_1 = -\mu < 0, \\
&\lambda_2 = \frac{\tau\Lambda}{M_2}(\frac{1}{R_0^m} - 1) + M_1(\frac{R_0^h}{R_0^m} - 1) = -\frac{\tau\Lambda}{M_2 R_0^m}(R_0^m - R_0^{mh}), \\
&\lambda_3 + \lambda_4 = -\frac{\Lambda\beta_2}{M_2} = -\mu R_0^m < 0,\ \lambda_3\lambda_4 = \Lambda\beta_2(1 - \frac{1}{R_0^m}),
\end{aligned}$$

It is evident that when $R_0^m < R_0^{mh}$, $\lambda_2 > 0$, and at this point, the equilibrium E_m^* is unstable. □

3.3.3. Stability analysis of the HFMD endemic equilibrium point E_h^*

Theorem 8. *When $0 < R_0^m < R_0^h$ and $1 < R_0^h < R_0^{mh}$, the hand-foot-and-mouth disease endemic equilibrium point E_h^* of system (1) is globally asymptotically stable. However, when $R_0^m > R_0^h > 1$, or $0 < R_0^m < R_0^h$ and $1 < R_0^{mh} < R_0^h$, the equilibrium point E_h^* becomes unstable.*

Proof. To prove this, we first construct a Lyapunov function:

$$V_h(t) = V_h(S(t), I_h(t), I_m(t)) = S_h^* g(\frac{S}{S_h^*}) + I_{hh}^* g(\frac{I_h}{I_{hh}^*}) + I_m$$

Next, we compute the total derivative of $V_h(t)$ along the trajectories of system (1), obtaining:

$$\begin{aligned}
\dot{V}_h(t) = \frac{d}{dt}V_h(t) &= (1 - \frac{S_h^*}{S})\frac{dS}{dt} + (1 - \frac{I_{hh}^*}{I_h})\frac{dI_h}{dt} + \frac{dI_m}{dt} \\
&= 2\Lambda - \Lambda\frac{S_h^*}{S} - (\mu + \beta_1 I_{hh}^*)S - (\beta_2 S_h^* + \tau I_{hh}^* - M_2)I_m \\
&\le 2\Lambda - 2\sqrt{(\mu + \beta_1 I_{hh}^*)\Lambda S_h^*} - (\beta_2 S_h^* + \tau I_{hh}^* - M_2)I_m \\
&= 2\Lambda - 2\Lambda - \frac{\Lambda\tau}{M_1 R_0^h}[(R_0^h - (1 + \frac{\Lambda\tau}{M_1 M_2}(R_0^h - R_0^m)]I_m \\
&= \frac{\Lambda\tau}{M_1 R_0^h}[(R_0^h - (1 + \frac{M_1 M_2}{\Lambda\tau}(R_0^h - R_0^m)]I_m \\
&= \frac{\Lambda\tau}{M_1 R_0^h}(R_0^h - R_0^{mh}) \le 0.
\end{aligned}$$

It is apparent that, under the conditions $1 < R_0^m < R_0^h$ and $1 < R_0^h < R_0^{mh}$, the derivative $\dot{V}_h(t) = 0$ if and only if $(S, I_h, I_m, R) = E_h^*$. Following the theoretical framework provided by LaSalle's Invariance Principle (as presented in Theorem 3), this implies that E_h^* is globally asymptotically stable within the invariant region Ω.

Now, we analyze the Jacobian matrix of the system (1) at the equilibrium point E_h^*:

$$J_h = Df(E_h^*) = \begin{bmatrix}
-\frac{\Lambda\beta_1}{M_1} & -M_1 & -\frac{\beta_2 M_1}{\beta_1} & 0 \\
\frac{\Lambda\beta_1}{M_1} - \mu & 0 & -\frac{\tau(\Lambda\beta_1 - \mu M_1)}{M_1\beta_1} & 0 \\
0 & 0 & \frac{\beta_2 M_1}{\beta_1} - \frac{\tau(\Lambda\beta_1 - \mu M_1)}{M_1\beta_1} - M_2 & 0 \\
0 & \theta_1 & \theta_2 & -\mu
\end{bmatrix}.$$

Let the eigenvalues of the Jacobian matrix J_h be denoted as λ_i (for $i = 1, 2, 3, 4$), where:

$$\begin{aligned}
\lambda_1 &= -\mu, \\
\lambda_2 &= \frac{\Lambda\beta_1\tau + M_1^2\beta_2 - M_1M_2\beta_1 - M_1\mu\tau}{M_1\beta_1} \\
&= \frac{\tau\Lambda}{R_0^h M_1}(R_0^h - 1 - \frac{M_1M_2}{\tau\Lambda}(R_0^h - R_0^m)) \\
&= \frac{\tau\Lambda}{R_0^h M_1}(R_0^h - R_0^{mh}), \\
\lambda_3 + \lambda_4 &= -\frac{\Lambda\beta_1}{M_1},\ \lambda_3\lambda_4 = \Lambda\beta_1 - \mu M_1 = \Lambda\beta_1(1 - \frac{1}{R_0^h}),
\end{aligned}$$

Thus, for the system to exhibit instability, we require that the eigenvalue $\lambda_2 > 0$. This occurs when either $R_0^h > 1$ and $R_0^m > R_0^h$, or $0 < R_0^m < R_0^h$ and $R_0^h > R_0^{mh} > 1$. Under these conditions, the equilibrium point E_h^* becomes unstable. □

3.3.4. Stability analysis of the HFMD-Measles endemic equilibrium point *E**

Since the fourth equation of system (1) is independent of the first three equations, when investigating its global stability, we only need to consider the following simplified system:

$$\begin{cases}
S' = \Lambda - \beta_1 S I_h - \beta_2 S I_m - \mu S, \\
I_h' = \beta_1 S I_h - (\theta_1 + d_1 + \mu) I_h - \tau I_h I_m, \\
I_m' = \beta_2 S I_m + \tau I_h I_m - (\theta_2 + d_2 + \mu) I_m
\end{cases} \tag{7}$$

Based on Theorem 2, it can be concluded that the system possesses a coexisting endemic equilibrium point $E_1^* = (S^*, I_h^*, I_m^*)$ when $0 < R_0^m < R_0^{mh} < R_0^h$. Furthermore, we obtain that

Theorem 9. *When $0 < R_0^m < R_0^{mh} < R_0^h$, the equilibrium point E_1^* of system (7) is globally asymptotically stable.*

Proof. We begin by constructing a Lyapunov function:

$$V(t) = V(S(t), I_h(t), I_m(t)) = S^* g(\frac{S}{S^*}) + I_h^* g(\frac{I_h}{I_h^*}) + I_m^* g(\frac{I_m}{I_m^*})$$

Next, we calculate the total derivative of $V(t)$ along the trajectory of system (7):

$$\begin{aligned}
\dot{V}(t) = \frac{d}{dt}V(t) &= (1 - \frac{S^*}{S})\frac{dS}{dt} + (1 - \frac{I_h^*}{I_h})\frac{dI_h}{dt} + (1 - \frac{I_m^*}{I_m})\frac{dI_m}{dt} \\
&= 2\Lambda - \Lambda\frac{S^*}{S} - (\beta_1 I_h^* + \beta_2 I_m^* + \mu)S.
\end{aligned}$$

According to the first equation of model (7), we obtain $S^*(\beta_1 I_h^* + \beta_2 I_m^* + \mu) = \Lambda$, then $\beta_1 I_h^* + \beta_2 I_m^* + \mu = \frac{\Lambda}{S^*}$, which leads to

$$\dot{V}(t) = 2\Lambda - \Lambda\frac{S^*}{S} - \Lambda\frac{S}{S^*} \leq 2\Lambda - 2\Lambda = 0.$$

A straightforward calculation shows that $\dot{V}(t) = 0$ if $S = S^*$. Substituting $S =$

S^* into the first equation of system (7), we obtain:

$$\Lambda - \beta_1 S^* I_h - \beta_2 S^* I_m - \mu S^* = 0 \tag{8}$$

Differentiating both sides of Equation (8) with respect to time t, we get:

$$(\beta_2 - \beta_1)\tau S^* I_h I_m - \beta_1 S^*(\beta_2 S^* - M_2) I_m - \beta_2 S^*(\beta_1 S^* - M_1) I_h = 0, \tag{9}$$

Given that $I_m, I_h > 0$, combining Equations (8) and (9), we can deduce that $I_m = I_m^*, I_h = I_h^*$. Thus, the conditions of Theorem 4 are satisfied, we conclude that when $0 < R_0^m < R_0^{mh} < R_0^h$, the equilibrium point (S^*, I_h^*, I_m^*) of system (7) is globally asymptotically stable. □

As established by the limiting system theory [25, 26], the global asymptotic stability of equilibrium point E_1^* in system (7) guarantees the global asymptotic stability of equilibrium point E^* in system (1). This theoretical foundation, combined with Theorem 9, yields the following conclusion:

Theorem 10. *When $0 < R_0^m < R_0^{mh} < R_0^h$, the Measle-HFMD endemic equilibrium point E^* of the co-infection model described by system (1) is globally asymptotically stable within the region Ω.*

4. Analysis of the $SI_hI_mI_{mh}R_mR_hR_{mh}$ epidemic model

Since the last three equations of system (2) are independent, we only need to analyze the following system to investigate its dynamic behavior.

$$\begin{cases} S' = \Lambda - \beta_1 S I_h - \beta_2 S I_m - (\beta_3 + \beta_4) S I_{mh} - \mu S \\ I_h' = \beta_1 S I_h + \beta_3 S I_{mh} - (\theta_1 + d_1 + \mu) I_h - \tau_1 I_h I_m \\ I_m' = \beta_2 S I_m + \beta_4 S I_{mh} - (\theta_2 + d_2 + \mu) I_m - \tau_2 I_m \\ I_{mh}' = \tau_1 I_h I_m + \tau_2 I_m - (\theta_3 + d_3 + \mu) I_{mh} \end{cases} \tag{10}$$

Similar to the discussion in Section 3.1.1, we find that system (10) has an invariant feasible region

$$\Sigma = \{(S, I_h, I_m, I_{mh}) \in R_+^4 \mid 0 \le S, I_h, I_m, I_{mh}, S + I_h + I_m + I_{mh} \le \tfrac{\Lambda}{\mu}\}.$$

4.1. Basic reproduction number of model (10)

System (10) also possesses a disease-free equilibrium point $\mathcal{E}_0 = (S_0, 0, 0, 0)$ with $S_0 = \frac{\Lambda}{\mu}$. Let $u = (I_h, I_m, I_{mh})$ represent the infected compartments of system (10). The corresponding infected subsystem can be described as:

$$\begin{aligned} I'_h &= \beta_1 S I_h + \beta_3 S I_{mh} - (\theta_1 + d_1 + \mu) I_h - \tau_1 I_h I_m, \\ I'_m &= \beta_2 S I_m + \beta_4 S I_{mh} - (\tau_2 + \theta_2 + d_2 + \mu) I_m, \\ I'_{mh} &= \tau_1 I_h I_m + \tau_2 I_m - (\theta_3 + d_3 + \mu) I_{mh} \end{aligned} \tag{11}$$

Taking $\mathcal{F}(u) = (\beta_1 S I_h + \beta_3 S I_{mh}, \beta_2 S I_m + \beta_4 S I_{mh}, 0)^T$ and

$$\mathcal{V}(u) = (m_1 I_h + \tau_1 I_h I_m, m_2 I_m, m_3 I_{mh} - \tau_1 I_h I_m - \tau_2 I_m)^T,$$

where $m_1 = (\theta_1 + d_1 + \mu), m_2 = (\theta_2 + d_2 + \mu), m_3 = (\theta_3 + d_3 + \mu)$.

Using the next-generation matrix method, the basic reproduction number of system (10) is obtained as

$$\mathcal{R}_0 = \max\{\mathcal{R}_0^h, \mathcal{R}_0^m\},$$

where $\mathcal{R}_0^h = \frac{\beta_1 \Lambda}{\mu m_1}$, and $\mathcal{R}_0^m = \frac{\Lambda(\beta_2 m_3 + \beta_4 \tau_2)}{\mu(m_2+\tau_2)m_3}$ denote the basic reproduction numbers for hand-foot-mouth disease and measles, respectively.

The Threshold Theorem developed by Van den Driessche and Watmough [22] states that the stability of the disease-free equilibrium is closely related to the basic reproduction number $\mathcal{R}_0$.

Theorem 11. *For system (10) , the disease-free equilibrium $\mathcal{E}_0$ is locally asymptotically stable if the basic reproduction number $\mathcal{R}_0$ is less than* 1*, whereas stability is lost when $\mathcal{R}_0$ surpasses* 1.

Proof. Linearizing the system at the disease-free equilibrium $\mathcal{E}_0$ yields the Jacobian matrix $\mathcal{J}_0$:

$$\mathcal{J}_0 = \begin{bmatrix} -\mu & -\frac{\beta_1\Lambda}{\mu} & -\frac{\Lambda\beta_2}{\mu} & -\frac{\Lambda(\beta_3+\beta_4)}{\mu} \\ 0 & \frac{\beta_1\Lambda}{\mu} - m_1 & 0 & \frac{\Lambda\beta_3}{\mu} \\ 0 & 0 & \frac{\Lambda\beta_2}{\mu} - m_2 - \tau_2 & \frac{\Lambda\beta_4}{\mu} \\ 0 & 0 & \tau_2 & -m_3 \end{bmatrix}$$

The eigenvalues satisfy $\lambda_1 = -\mu$ and

$$\lambda_2 = \frac{\Lambda\beta_1}{\mu} - m_1 = m_1\left(R_0^h - 1\right),$$

while the remaining two eigenvalues λ_3 and λ_4 obey:

$$\lambda_3 + \lambda_4 = -\frac{\beta_2\Lambda}{\mu} + (m_2 + m_3 + \tau_2) = (1 - R_0^m)(m_2 + \tau_2) + \frac{\beta_4\Lambda\tau_2}{\mu m_3} + m_3,$$
$$\lambda_3\lambda_4 = -m_3(\frac{\Lambda\beta_2}{\mu} - m_2 - \tau_2) = m_3(m_2 + \tau_2)(1 - R_0^m).$$

When the basic reproduction number $\mathcal{R}_0 < 1$, all eigenvalues have negative real parts, indicating system stability. If $\mathcal{R}_0 > 1$, either the $\mathcal{R}_0^h > 1$ or $\mathcal{R}_0^m > 1$, resulting in at least one eigenvalue with positive real part and consequent instability of $\mathcal{E}_0$. □

4.2. Global asymptotic stability of the disease-free equilibrium $\mathcal{E}_0$

To investigate the global stability of the disease-free equilibrium, we define the parameter

$$\tilde{\mathcal{R}}_0 = \max\{\mathcal{R}_0^h, \tilde{\mathcal{R}}_0^m, \tilde{\mathcal{R}}_0^{mh}\},$$

where $\tilde{\mathcal{R}}_0^m = \frac{\Lambda\beta_2}{\mu m_2}$ and $\tilde{\mathcal{R}}_0^{mh} = \frac{\Lambda(\beta_3+\beta_4)}{\mu m_3}$.

Theorem 12. *When $\tilde{\mathcal{R}}_0 < 1$, the disease-free equilibrium $\mathcal{E}_0$ of the system (10) is globally asymptotically stable in the domain Σ .*

Proof. For the disease-free equilibrium $\mathcal{E}_0$ of the system (10), we construct the Lyapunov function:

$$\mathcal{V}_0(t) = \mathcal{V}_0(S(t), I_h(t), I_m(t), I_{mh}(t)) = S^0 g(\tfrac{S}{S^0}) + I_h + I_m + I_{mh}.$$

By calculating the total derivative of $\frac{d\mathcal{V}_0}{dt}$ along the trajectories of the system :

$$\begin{aligned}\dot{\mathcal{V}}_0(t) &= \frac{d}{dt}\mathcal{V}_0(t) = (1-\frac{S^0}{S})\frac{dS}{dt} + \frac{dI_h}{dt} + \frac{dI_m}{dt} + \frac{dI_{mh}}{dt} \\ &= (\frac{\Lambda\beta_1}{\mu} - m_1)I_h + (\frac{\Lambda\beta_2}{\mu} - m_2)I_m + (\frac{\Lambda(\beta_3+\beta_4)}{\mu} - m_3)I_{mh} \\ &\quad + \Lambda(2 - \frac{S}{S_0} - \frac{S_0}{S}).\end{aligned}$$

Based on the definition of $\tilde{\mathcal{R}}_0$, we can further deduce that

$$\begin{aligned}\dot{\mathcal{V}}_0(t) &= m_1 I_h(\mathcal{R}_0^h - 1) + m_2 I_m(\tilde{\mathcal{R}}_0^m - 1) + m_3(\tilde{\mathcal{R}}_0^{mh} - 1)I_{mh} \\ &\quad + \Lambda(2 - \frac{S}{S_0} - \frac{S_0}{S}).\end{aligned}$$

Since $\tilde{\mathcal{R}}_0 < 1$, it follows that $\mathcal{R}_0^h < 1$, $\tilde{\mathcal{R}}_0^m < 1$ and $\tilde{\mathcal{R}}_0^{mh} < 1$, leading to $\dot{\mathcal{V}}_0(t) \leq 0$. Clearly, $\dot{\mathcal{V}}_0(t) = 0$ holds if and only if $S = S_0, I_h = I_m = I_{mh} = 0$. By applying LaSalle's Invariance Principle (Theorem 3), the disease-free equilibrium point $\mathcal{E}_0$ of the system (10) is globally asymptotically stable in Σ. □

Since $\mathcal{R}_0 \leq \tilde{\mathcal{R}}_0$, there is a gap between the conditions $\mathcal{R}_0 \leq 1$ and $\mathcal{R}_0^h \leq 1$. A natural question is:

Problem 1. *When $\mathcal{R}_0 \leq 1$, is the disease-free equilibrium $\mathcal{E}_0$ of system (10) globally asymptotically stable?*

To further explore this issue, we consider the cases where $\beta_3 = 0$ or $\beta_4 = 0$. If $\beta_3 = 0$, system (10) simplifies to the following system:

$$\begin{cases} S' = \Lambda - \beta_1 S I_h - \beta_2 S I_m - \beta_4 S I_{mh} - \mu S \\ I_h' = \beta_1 S I_h - (\theta_1 + d_1 + \mu) I_h - \tau_1 I_h I_m \\ I_m' = \beta_2 S I_m + \beta_4 S I_{mh} - (\theta_2 + d_2 + \mu) I_m - \tau_2 I_m \\ I_{mh}' = \tau_1 I_h I_m + \tau_2 I_m - (\theta_3 + d_3 + \mu) I_{mh} \end{cases} \tag{12}$$

Theorem 13. *When $\mathcal{R}_0 \leq 1$, the disease-free equilibrium $\mathcal{E}_0$ of system (12) is globally asymptotically stable within region Σ.*

Proof. Considering the positive invariance of region Σ, according to the second equation of system (12):

$$I_h' = \beta_1 S I_h - (\theta_1 + d_1 + \mu) I_h - \tau_1 I_h I_m \leq (\beta_1 S_0 - m_1) I_h = m_1(\frac{\beta_1 S_0}{m_1} - 1) I_h,$$

thus if $\mathcal{R}_0 \leq 1$, $I_h(t) \to 0$ as $t \to +\infty$, at which point the limit system of system (12) is

$$\begin{cases} S' = \Lambda - \beta_2 S I_m - \beta_4 S I_{mh} - \mu S \\ I_m' = \beta_2 S I_m + \beta_4 S I_{mh} - (\tau_2 + m_2) I_m \\ I_{mh}' = \tau_2 I_m - m_3 I_{mh} \end{cases} \tag{13}$$

As can be readily observed, the system described by (13) admits an equilibrium solution at $\mathbb{E}_0 = (S_0, 0, 0)$. Similar to the proof of the Theorem 11, the equilibrium

point $\mathbb{E}_0$ of model (13) is locally asymptotically stable.

Due to the condition $S \leq S_0$, the last pair of equations in the system are:

$$\begin{cases} I'_m \leq (\beta_2 S_0 - \tau_2 - m_2) I_m + \beta_4 S_0 I_{mh} \\ I'_{mh} = \tau_2 I_m - m_3 I_{mh} \end{cases} \tag{14}$$

Consider the auxiliary system

$$\begin{cases} \bar{I}'_m = (\beta_2 S_0 - \tau_2 - m_2) \bar{I}_m + \beta_4 S_0 \bar{I}_{mh} \\ \bar{I}'_{mh} = \tau_2 \bar{I}_m - m_3 \bar{I}_{mh} \end{cases} \tag{15}$$

This linear system has two characteristic roots $\tilde{\lambda}_1, \tilde{\lambda}_2$ satisfying

$$\begin{aligned} &\tilde{\lambda}_1 \tilde{\lambda}_2 = m_3 (1 - R_0^m)(m_2 + \tau_2) \\ &\tilde{\lambda}_1 + \tilde{\lambda}_2 = (R_0^m - 1)(m_2 + \tau_2) - \frac{\beta_4 \tau_2 \Lambda}{\mu m_3} - m_3 \end{aligned} \tag{16}$$

Therefore, if $\mathcal{R}_0 < 1$, both roots must have negative real parts, which leads to $\bar{I}_m \to 0$ and $\bar{I}_{mh} \to 0$ as t tends to $+\infty$.

According to the comparison theorem, $I_m \to 0$ and $I_{mh} \to 0$ as t tends to $+\infty$. At this point, we obtain the limiting system of model (13) as

$$S' = \Lambda - \mu S \tag{17}$$

It is clear that $\lim_{t \to +\infty} S(t) = S_0$, and the equilibrium S_0 of model (17) is globally asymptotically stable. Following the limiting system theory, model (13) is globally attractive.

In addition, the Jacobian matrix of system (13) at $\mathbb{E}_0$:

$$J_{\mathbb{E}_0} = \begin{bmatrix} -\mu & -\frac{\Lambda \beta_2}{\mu} & -\frac{\beta_4 \Lambda}{\mu} \\ 0 & \frac{\Lambda \beta_2}{\mu} - m_2 - \tau_2 & \frac{\beta_4 \Lambda}{\mu} \\ 0 & \tau_2 & -m_3 \end{bmatrix}.$$

From (16), when $\mathcal{R}_0 < 1$, the Jacobian $J_{\mathbb{E}_0}$ has eigenvalues satisfying $\mathrm{Re}(\tilde{\lambda}_i) < 0, (i = 1, 2)$, and $\tilde{\lambda}_3 = -\mu < 0$, that is, $\mathbb{E}_0$ is locally asymptotically stable, and it can be obtained that the limit system (13) is globally asymptotically stable. According to the limit system theory, we can obtain that the disease-free equilibrium $\mathcal{E}_0$ of the system (12) is globally asymptotically stable. □

Based on a method analogous to the proof process of Theorem 12, the following conclusion can be obtained:

Theorem 14. *When $\mathcal{R}_0 \leq 1$, the disease-free equilibrium $\mathcal{E}_0$ of system (12) is globally asymptotically stable within Σ under the condition of $\beta_3 \beta_4 = 0$.*

5. Numerical simulations and data fitting

5.1. Numerical simulations of SI_hI_mR epidemic model (1)

In order to verify the accuracy of the theoretical analysis, numerical simulations are employed in this section.

The parameters presented in **Table 3** yield values of $R_0^h \approx 0.375$ and $R_0^m \approx 0.25$ with the corresponding solution curve illustrated in **Figure 4**. As the system (1) evolves over time, the number of infected individuals gradually decreases to zero, suggesting that the disease will not become endemic but will eventually be eradicated. This observation serves as a validation of the correctness of the Theorem 6.

Table 3. Parameter values when $R_0 < 1$.

Parameters	Λ	β_1	β_2	μ	θ_1	θ_2	d_1	d_2	τ
Values	0.8	0.15	0.01	0.2	0.3	0.2	0.1	0.2	0.5

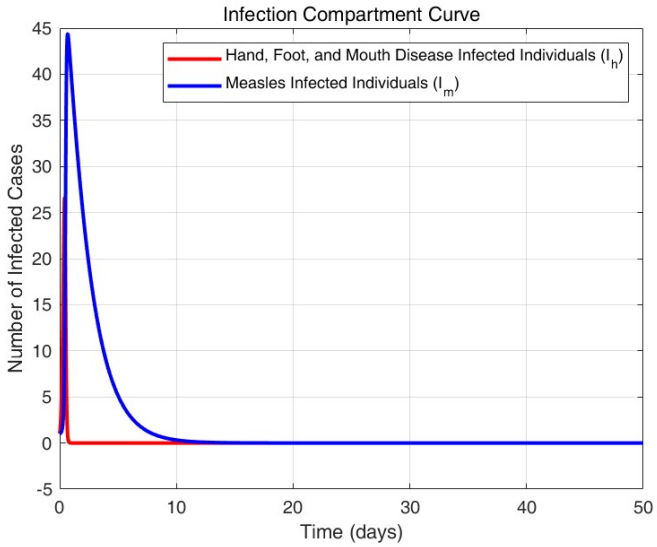

Figure 4. Solution curves at $R_0^h \approx 0.375, R_0^m \approx 0.25$

The parameters in **Table 4** yield values of $R_0^h \approx 0.9$ and $R_0^m \approx 4.5$, with the corresponding solution curve shown in **Figure 5**. As the system (1) evolves over time, the number of hand, foot, and mouth disease cases gradually approaches zero, while the measles disease transitions into an endemic state. This outcome confirms the validity of the Theorem 7.

Table 4. Parameter values when $R_0^m > 1 > R_0^h$

Parameters	Λ	β_1	β_2	μ	θ_1	θ_2	d_1	d_2	τ
Values	4	0.1	0.5	0.4	0.4	0.5	0.25	0.2	0.1

The parameters in **Table 5** are $R_0^h \approx 8.3$ and $R_0^m \approx 0.9$, with the corresponding solution curve shown in **Figure 6**. As the system (1) evolves over time, the number of measles cases gradually decreases to zero, while the hand, foot, and mouth disease

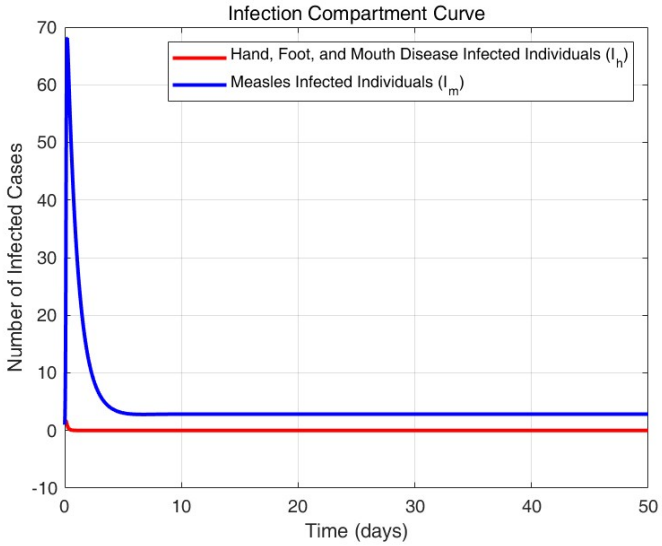

Figure 5. Solution curves at $R_0^h \approx 0.9$,$R_0^m \approx 4.5$

transitions into an endemic state. This outcome further validates the correctness of the Theorem 8.

Table 5. Parameter values when $R_0^h > 1 > R_0^m$.

Parameters	Λ	β_1	β_2	μ	θ_1	θ_2	d_1	d_2	τ
Values	4	0.5	0.1	0.4	0.1	0.5	0.1	0.2	0.1

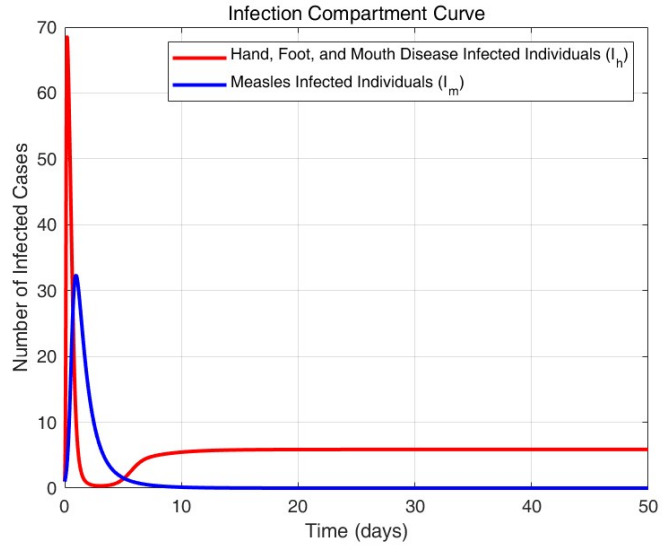

Figure 6. Solution curves at $R_0^h \approx 8.3$, $R_0^m \approx 0.9$.

The parameters in **Table 6** are $R_0^h \approx 13.3$, $R_0^m \approx 0.9$, and $R_0^{mh} \approx 1.8$, yielding the relationship $R_0^h > R_0^{mh} > 1 > R_0^m$. The corresponding solution curve is shown in **Figure 7**. As the system (1) evolves over time, both measles and hand, foot, and mouth disease become endemic. This result serves to confirm the validity of Theorem 9.

Table 6. Parameter values when $R_0^h > R_0^{mh} > 1 > R_0^m$.

Parameters	Λ	β_1	β_2	μ	θ_1	θ_2	d_1	d_2	τ
Values	8	0.4	0.05	0.4	0.1	0.5	0.1	0.2	0.1

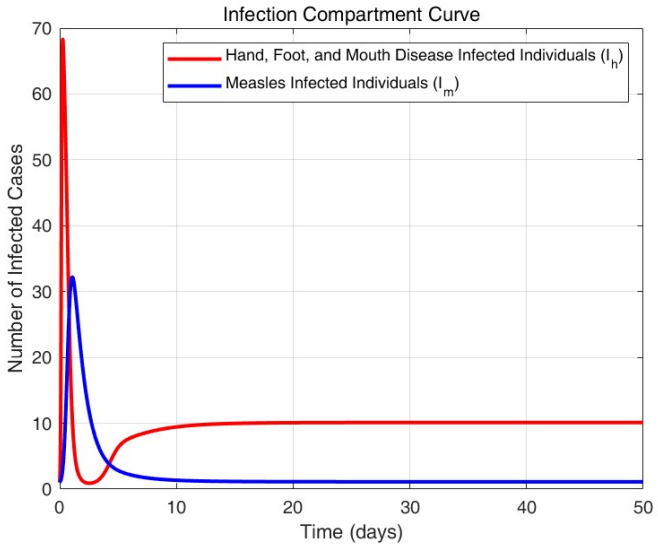

Figure 7. Solution curves at $R_0^h \approx 13.3, R_0^m \approx 0.9, R_0^{mh} \approx 1.8$.

5.2. Model fitting and verification of co-infection model (2)

To validate the rationality of the $SI_hI_mI_{mh}R_hR_mR_{mh}$ model (2), this study selects measles and hand-foot-mouth disease (HFMD) epidemic data from February to September 2024 in mainland China and employs the least squares method for fitting.

5.2.1. Data collection

The data were obtained from the Chinese Center for Disease Control and Prevention (https://www.chinacdc.cn/jksj/jksj01/), covering real-time epidemic data from February to September 2024. The total population of China is approximately 1.4 billion. Based on the CDC's official reports and the epidemiological characteristics of measles and HFMD, the susceptible population was assumed to primarily consist of unvaccinated children or individuals with vaccine failure, accounting for about 1% of the total population. The initial values for the model are listed in **Table 7**, with the initial time t_0 set to February 2024.

5.2.2. Objective function

Given that the last three equations of model (2) are independent of each other, to facilitate data fitting, we focus on the simplified model:

$$\begin{cases} S' = \Lambda - \beta_1 SI_h - \beta_2 SI_m - (\beta_3 + \beta_4) SI_{mh} - \mu S, \\ I_h' = \beta_1 SI_h + \beta_3 SI_{mh} - m_1 I_h - \tau_1 I_h I_m, \\ I_m' = \beta_2 SI_m + \beta_4 SI_{mh} - m_2 I_m - \tau_2 I_m, \\ I_{mh}' = \tau_1 I_h I_m + \tau_2 I_m - m_3 I_{mh} \end{cases} \tag{18}$$

where $m_i (i = 1, 2, 3)$ is defined in Section 4.1.

Parameter estimation was performed using the 'lsqcurvefit' function in MATLAB. Following the idea of Fandio et al. [27], the objective function is defined as:

$$F(\Theta) = \sum_{i=1}^{8} \left((I_m^{data}(t_i) - I_m(t_i))^2 + (I_h^{data}(t_i) - I_h(t_i))^2 \right)$$

where $\Theta = (\beta_1, \beta_2, \beta_3, \beta_4, m_1, m_2, m_3, \tau_1, \tau_2, \mu, \Lambda)$, $I_m^{data}(t_i)$ and $I_h^{data}(t_i)$ represent the actual data for measles and HFMD, respectively, and $I_m(t_i)$ and $I_h(t_i)$ denote the fitted data.

5.2.3. Model validation

The coefficient of determination (R^2) and mean absolute percentage error ($MAPE$) are used to evaluate the fitting performance, defined as:

$$R^2 = 1 - \frac{\sum_{i=1}^{n}(y_i - \hat{y}_i)^2}{\sum_{i=1}^{n}(y_i - \bar{y})^2}, \quad \text{MAPE} = \frac{100\%}{n} \sum_{i=1}^{n} \left| \frac{\hat{y}_i - y_i}{y_i} \right|$$

Here, $y = (y_1, y_2, \ldots, y_n)$ represents the observed data, $\hat{y} = (\hat{y}_1, \hat{y}_2, \ldots, \hat{y}_n)$ denotes the fitted data, and $\bar{y}$ is the mean of the observed data. A higher R^2 (closer to 1) and a lower MAPE (closer to 0) indicate better model performance.

5.2.4. Parameter estimation

The co-infection dynamics model (18) was calibrated using surveillance data of measles and HFMD outbreaks in mainland China from February to September 2024.

As demonstrated in **Tables 7** and **8** and the fitting curve in **Figure 8**, the fitting results of the HFMD and measles epidemic models in mainland China, where the curves show an excellent agreement with the observed data (HFMD: $R^2 = 0.986$, $MAPE = 19.8\%$; measles: $R^2 = 0.86$, $MAPE = 10.6\%$). These findings demonstrate that the differential equation-based model (18) accurately captures the transmission dynamics during specific outbreak phases.

Table 7. Initial values of model.

Variable	Estimated value	source	Variable	Estimated value	source
$S(0)$	13.68 million	estimate	$I_h(0)$	9093	CDC
$I_m(0)$	31	CDC	$I_{mh}(0)$	0	estimate

Table 8. Initial values of model (18).

Variable	Estimated value	source	Variable	Estimated value	source
β_1	0.5394	Estimate	β_2	0.2521	Estimate
β_3	0.0701	Estimate	β_4	0.0264	Estimate
m_1	6.3556	Estimate	m_2	2.8801	Estimate
m_3	0.0331	Estimate	τ_1	0.0184	Estimate
μ	0.0004	Estimate	Λ	0.2391	Estimate

The HFMD prediction model demonstrates a high goodness-of-fit ($R^2 = 0.986$), accounting for 98.6% of case variations. However, its MAPE of 19.8% indicates an average prediction deviation of nearly 20%. This discrepancy is likely attributed to

the strong seasonality of HFMD and the high underreporting rate of asymptomatic infections, particularly during peak outbreaks in summer and autumn in China, where mild or asymptomatic cases often go unrecorded, increasing prediction errors. In contrast, the measles model, despite its lower $R^2 = 0.86$, achieves a lower MAPE of 10.6%, indicating more accurate epidemic scale predictions. Measles control in China heavily relies on high vaccine coverage, making its transmission pattern more predictable and further affirming the crucial role of immunization in measles containment.

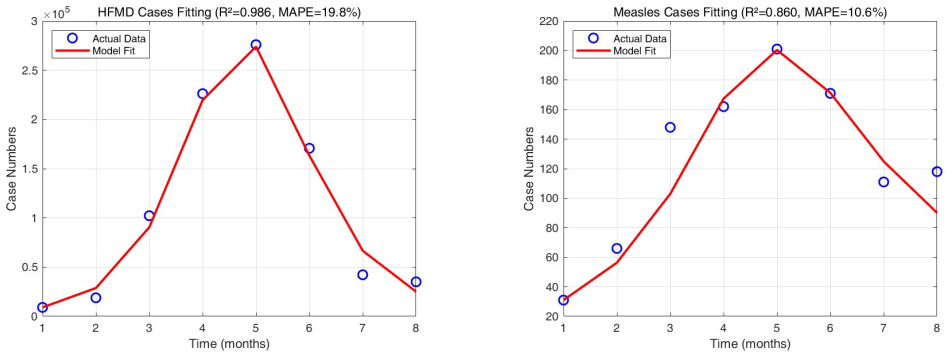

(a) Fitting curves for the cases of HFMD **(b)** Fitting curves for the cases of Measles

Figure 8. Fitting results of the co-infection model (18).

6. Concluding remarks

This study investigates the co-dynamics of measles and hand, foot, and mouth disease (HFMD) by constructing two epidemiological models: a four-compartment SI_hI_mR model and a seven-compartment $SI_hI_mI_{mh}R_hR_mR_{mh}$ co-infection model. The dynamic behaviors of both models were thoroughly examined.

In the case of SI_hI_mR model with the four compartments, using the next-generation matrix approach, the basic reproduction numbers R_0^h for measles and R_0^m for HFMD are calculated. By examining the correlation between R_0^h and R_0^m, the presence of equilibrium points is confirmed, with specific details depicted in **Figure 3**.

By applying LaSalle's invariance principle, the global asymptotic stability of these equilibrium points has been established. The specific stability regions are illustrated in **Figure 9** and **Table 1**, where $W^s_{E_0}$, $W^s_{E_h^*}$, $W^s_{E_m^*}$ and $W^s_{E^*}$, denote the stability regions of equilibrium points E_0, E_h^*, E_m^*, and E^*, respectively.

These regions are mathematically defined as:

$$
\begin{aligned}
&W^s_{E_0} = \{(R_0^m, R_0^h) \in R_+^2 | 0 < R_0^m < 1, 0 < R_0^h < 1\},\\
&W^s_{E_m^*} = \{(R_0^m, R_0^h) \in R_+^2 | 0 < R_0^h < 1 < R_0^m \text{ or } 1 < R_0^{mh} < R_0^m < R_0^h\},\\
&W^s_{E_h^*} = \{(R_0^m, R_0^h) \in R_+^2 | 0 < R_0^m < R_0^h, 1 < R_0^h < R_0^{mh}\},\\
&W^s_{E^*} = \{(R_0^m, R_0^h) \in R_+^2 | 0 < R_0^m < R_0^{mh} < R_0^h\}.
\end{aligned}
$$

Our analysis reveals that when $R_0 = \max\{R_0^h, R_0^m\} < 1$, that is, $(R_0^h, R_0^m) \in W^s_{E_0}$, both measles and HFMD will eventually vanish, preventing any epidemic outbreak in the region. When $(R_0^m, R_0^h) \in W^s_{E_m^*}$, HFMD will diminish while measles

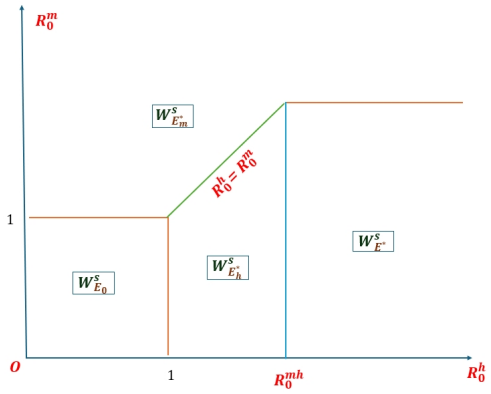

Figure 9. Stability regions of equilibria E_0, E_h^*, E_m^* and E^* of the SI_hI_mR model.

will persist endemically. Conversely, when $(R_0^m, R_0^h) \in W^s_{E_h^*}$, measles will disappear and HFMD will persist endemically. Moreover, when $(R_0^m, R_0^h) \in W^s_{E^*}$, both diseases will coexist and establish endemicity. Numerical simulations have validated the stability of these results.

For the $SI_hI_mI_{mh}R_hR_mR_{mh}$ model with seven compartments, the basic reproduction number $\mathcal{R}_0$ was calculated, and the threshold theorem was validated. Conditions for both local and global asymptotic stability of the disease-free equilibrium were established. Specifically, the disease-free equilibrium $\mathcal{E}_0$ is asymptotically stable when $\mathcal{R}_0 < 1$ and globally asymptotically stable when $\tilde{\mathcal{R}}_0 < 1$. However, a gap between these conditions remains unresolved and will be addressed in future research (**Figure 10**).

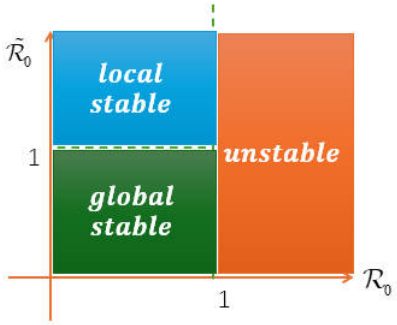

Figure 10. Stability regions of disease free equilibrium $\mathcal{E}_0$ of model .

Additionally, the existence and stability of endemic equilibria will be investigated in subsequent studies. The model's limitations, such as the exclusion of quarantine and treatment strategies' potential effects on cure rates and the possible implementation of measles vaccination programs to enhance disease resistance, will also be explored in future research.

Author contributions: Conceptualization, GL, LD and YM; methodology, GL, LD and YM; software, GL , LD and LC; validation, GL, LD and LC; formal analysis, GL, LD and YM; investigation, GL and LC; resources, GL and LD; data curation, GL and LD; writing-original draft preparation, GL and LD; writing—review and editing, GL and LD; visualization, GL and LD; supervision, GL; project administration, GL;

funding acquisition, GL. All authors have read and agreed to the published version of the manuscript.

Institutional review board statement: Not applicable.

Informed consent statement: Not applicable.

Funding: This research was partially supported by the Scientific and Technological Research Program of Chongqing Municipal Education Commission (Grant No. KJQN20180113) and was supported by Zhejiang Provincial Natural Science Foundation of China under Grant No. LZ23A010003. Additionally, it was funded by the Research Fund for the China Postdoctoral Science Foundation (Grant No. 2020M673166).

Conflict of interest: The authors declare no conflict of interest.

References

1. Perry RT, Halsey NA. The clinical significance of measles: A review. J. Infect. Dis. 2004; 189: S4–S16.
2. Vitek CR, Aduddell M, Brinton MJ, et al. Increased protections during a measles outbreak of children previously vaccinated with a second dose of measles mumps and rubella vaccine. Pediatr. Infect. Dis. J. 1999; 18(7): 620–623.
3. Carazo S, Billard MN, Boutin A, De Serres G. Effect of age at vaccination on the measles vaccine effectiveness and immunogenicity: Systematic review and meta-analysis. BMC Infectious Diseases. 2020; 20: 1–18.
4. Do LAH, Toh ZQ, Licciardi PV, et al. Can early measles vaccination control both measles and respiratory syncytial virus infections? The Lancet Global Health. 2022; 10(2): e288–e292.
5. Azam JM, Saitta B, Bonner K, et al. Modelling the relative benefits of using the measles vaccine outside cold chain for outbreak response. Vaccine. 2021; 39(39): 5845–5853.
6. Xue Y, Ruan X, Xiao Y. Measles dynamics on network models with optimal control strategies. Advances in Difference Equations. 2021; 2021(1): 138.
7. Ibrahim MA, Dénes A. Stability and threshold dynamics in a seasonal mathematical model for measles outbreaks with double-dose vaccination. Mathematics. 2023; 11(8): 1791.
8. Peter OJ, Panigoro HS, Ibrahim MA, et al. Analysis and dynamics of measles with control strategies: a mathematical modeling approach. International Journal of Dynamics and Control. 2023; 11(11): 2538–2552.
9. Ahmad W, Butt AIK, Rafiq M, et al. Modeling, analyzing and simulating the measles transmission dynamics through efficient computational optimal control technique. European Physical Journal Plus. 2024; 139(566).
10. Berhe HW, Gebremeskel AA, Atsbaha HA, et al. Modelling and stability analysis of the dynamics of measles with application to Ethiopian data. Heliyon. 2024; 10(e33594).
11. Arsal SR, Aldila D, Handari BD. Short review of mathematical model of measles. AIP Conf. Proc. 2020; 2264(1): 020003.
12. Ma YJ, Liu MX, Hou Q, et al. Modelling seasonal HFMD with the recessive infection in Shandong, China. Mathematical Biosciences and Engineering. 2013; 10(4): 1159–1171.
13. Wang JY, Xiao YN, Peng ZH. Modelling seasonal HFMD infections with the effects of contaminated environments in Chinese mainland. Applied Mathematics and Computation. 2016; 274: 615–627.
14. Wang JY, Xiao YN, Cheke RA. Modelling the effects of contaminated environments on seasonal HFMD infections and the potential benefit of a pulse vaccination strategy. Discrete & Continuous Dynamical Systems-B. 2017; 22(11): 1–22.
15. Zhang TR, Zhang ZJ, Yu ZY, et al. Effects of behaviour change on HFMD transmission. Journal of Biological Dynamics. 2023; 17(1): 2244968.
16. De Moraes-Pinto MI. Interaction between pediatric HIV infection and measles. Future Virology. 2011; 6(12): 1471–1479.
17. Berhe HW, Makinde OD, Theuri DM. Co-dynamics of measles and dysentery diarrhea diseases with optimal control and cost-effectiveness analysis. Applied Mathematics and Computation. 2019; 347: 903–921
18. Zhang J. Nursing Care for a Child with Hand-Foot-Mouth Disease Complicated by Measles and Pneumonia (In

Chinese). Contemporary Nurse (Lower Fortnightly Edition). 2019; 26(04): 151–152.
19. Chen S, Ran Y, Huang H, et al. Epidemic Dynamics of Two-Pathogen Spreading for Pairwise Models. Mathematics. 2022; 10: 1906.
20. Smith HL, Waltman P. The theory of the chemostat: dynamics of microbial competition. Cambridge University Press; 1995.
21. Lu GC, Lu ZY. Geometric criteria for the stability of high-dimensional systems (In Chinese). Science Press; 2019.
22. Van den Driessche P, Watmough J. Reproduction numbers and sub-threshold endemic equilibria for compartmental models of disease transmission. Mathematical Biosciences. 2002; 180(1–2): 29–48.
23. Martcheva M. An introduction to mathematical epidemiology. Springer; 2015.
24. LaSalle JP. The stability of dynamical systems. SIAM; 1976.
25. Thieme HR. Convergence results and a Poincaré-Bendixson trichotomy for asymptotically autonomous differential equations. J. Math. Biol. 1992; 30: 755–763.
26. Zhang J, Ma Z. Global dynamics of an SEIR epidemic model with saturating contact rate. Math Biosci. 2003; (185): 15–32.
27. Fandio R, Abboubakar H, Fouda HPE, et al. Mathematical modelling and projection of Buruli ulcer transmission dynamics using classical and fractional derivatives: A case study of Cameroon. Partial Differential Equations in Applied Mathematics. 2023; 8: 100589.